Sensors and Actuators A 238 (2016) 25–36

Contents lists available at ScienceDirect

Sensors and Actuators A: Physical

journal homepage: www.elsevier.com/locate/sna

Magnetostrictive type inductive sensing pressure sensor

Heng-Chung Chang[a], Sheng-Chieh Liao[b], Hsieh-Shen Hsieh[a], Jung-Hung Wen[c], Chih-Huang Lai[b], Weileun Fang[a,c,*]

[a] Power Mechanical Engineering, National Tsing Hua University, Hsinchu, Taiwan
[b] Materials Science & Engineering, National Tsing Hua University, Hsinchu, Taiwan
[c] Institute of NanoEngineering and MicroSystems, National Tsing Hua University, Hsinchu, Taiwan

ARTICLE INFO

Article history:
Received 3 September 2015
Received in revised form 29 October 2015
Accepted 19 November 2015
Available online 27 November 2015

Keywords:
Pressure sensor
Inverse-magnetostriction effect
Inductive sensing
CoFeB
Gauge factor

ABSTRACT

This study presents a magnetostrictive type inductive sensing pressure sensor which consisted of a planar coil, CoFeB magnetic films, and a Si diaphragm. As the Si diaphragm deformed by a pressure load, the inverse-magnetostriction effect would cause permeability changes of the CoFeB magnetic films. Thus, the permeability changes as well as the pressure load can be detected by the inductance change of a planar inductor. To demonstrate the feasibility of the proposed pressure sensor, the planar inductor designs of different coil turns and in-plane patterns of magnetic films are fabricated and tested. Preliminary measurements show that the pressure sensors with 6 and 12 coil turns have sensitivities of 0.079 %/kPa and 0.064 %/kPa, respectively. In addition, based on the in-plane pattern design of the magnetic films, the gauge factor could be tuned from 55 to 852.

1. Introduction

The demand of pressure sensors has been continuously increasing recently, for instance, pressure sensors have been extensively exploited for the tire pressure and blood pressure monitoring, and also the altimeter for the personal navigation. In general, the sensing approaches of pressure sensors can be categorized as: piezoresistive, capacitive, and piezoelectric [1,2]. The piezoresistive sensing element is the most popular approach for the silicon pressure sensor [2,3]. By using existing process technologies and materials, piezoresistors are implemented and integrated with a sensing diaphragm. The gauge factor of the silicon-based piezoresistive type pressure sensor is around 70–110 [4]. The gauge factor can be improved by reducing the doping concentration of the piezoresistor, however the temperature stability of the sensor is decreased [5].

The inverse-magnetostriction effect (Villari effect) has been investigated and reported in [6–8]. The investigations indicate that permeability of a magnetic material can be changed by an external load. The Villari effect has been exploited to develop the magnetic tunnel junction (MTJ) devices for the applications of gauge or pressure sensors [9–12]. Typically, the CoFeB film used in these MTJ devices has advantages of high gauge factor and excellent temperature stability [13,14]. However, unique facilities are required to prepare an additional pinning film during the process. The inductive sensing mechanism is also employed for a better sensitivity. The inductance variation could be read out by an inductive voltage or an oscillator circuit which converts the inductance of a coil to the frequency [15,16]. The inductance sensing could also enable the wireless transmission of sensing signals. The wireless transmission could bring a positive impact for some medical applications, such as the intraocular pressure monitoring [17,18]. Nevertheless, the bulky inductive sensing module is still a concern for various applications.

This study proposes a pressure sensor consisted of a planar coil with magnetic films to couple the inverse-magnetostrictive effect and the inductive sensing. In this design, a pressure load will change the permeability of the magnetic films due to the inverse-magnetostriction effect. As a result, the inductance of the planar coil disposed between the magnetic films will be changed and thus the pressure load can be measured by the inductance variation. The special equipment for the pinning layer of the MTJ device is not required for the proposed design. Moreover, a compact inductive sensing device can be achieved via the vertical integration of the planar coil and the magnetic films. Based on this sensing mechanism, the magnetostrictive type inductive sensing pressure sensors with various planar inductor designs are investigated. The gauge factor could be further modified by design parameters of the planar inductor, including the coil turns and the in-plane patterns of

* Corresponding author at: Power Mechanical Engineering, National Tsing Hua University, Hsinchu, Taiwan. Tel: +886 3 5742923; fax: +886 3 5739372.
E-mail address: fang@pme.nthu.edu.tw (W. Fang).

http://dx.doi.org/10.1016/j.sna.2015.11.023
0924-4247/

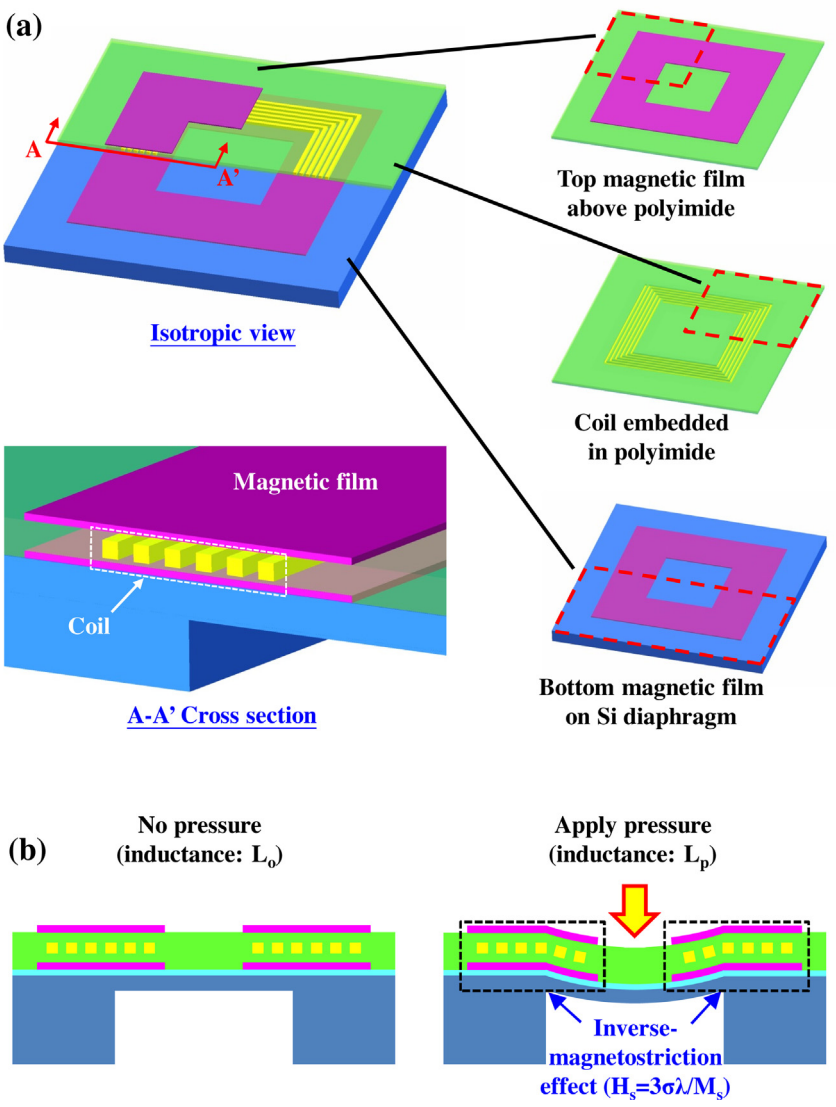

Fig. 1. The design concept of the magnetostrictive type pressure sensor, (a) structure schema, (b) sensing mechanism.

the magnetic films. Thus, the proposed designs can be implemented using the existing micro fabrication processes.

2. Concept and design

Fig. 1 illustrates the pressure sensor design formed by the proposed magnetic sensing unit on top of a deformable diaphragm. As depicted in Fig. 1(a), the proposed magnetic sensing unit mainly consists of a planar coil and two magnetic films (CoFeB film is employed in this study). The planar coil is sandwiched between these two magnetic films. The polyimide is employed as a filling material between the coil and the CoFeB films for an electrical isolation. By the integration of the planar coil, two magnetic films, and the polyimide layer, a planar inductor is constructed. The number of coil turns defined by the photolithography could modulate the initial inductance L_o of the planar inductor. Fig. 1(b) further illustrates the sensing principle of the proposed pressure sensor. As shown in the left illustration, the sensor has an initial inductance of L_o before applying a pressure load. As depicted in the right illustration, the diaphragm of sensor is deformed after applying the pressure load. The CoFeB magnetic films on the deformed diaphragm are then under a stress σ . According to the inverse-magnetostriction effect [13], the magnetic anisotropy field H_s of the CoFeB film induced by the stress σ can be expressed as,

$$H_s = \frac{3\sigma\lambda}{M_s} \tag{1}$$

where λ and M_s are respectively the magnetostriction constant and the saturation magnetization (in emu/cm^3) of the CoFeB film. In addition, the permeability μ of the magnetic film is expressed as [19],

$$\mu = \frac{4\pi M_s}{H_o - H_s} \tag{2}$$

where H_o is the anisotropy field of the magnetic film before the stress σ applying on the film. The parameter H_o could be controlled by the deposition process or in-plane pattern designs of the magnetic films. By combining Eqs. (1) and (2), the relation between the permeability μ and the stress σ on the magnetic film is expressed as,

$$\mu = \frac{4\pi {M_s}^2}{M_s H_o - 3\sigma\lambda} \tag{3}$$

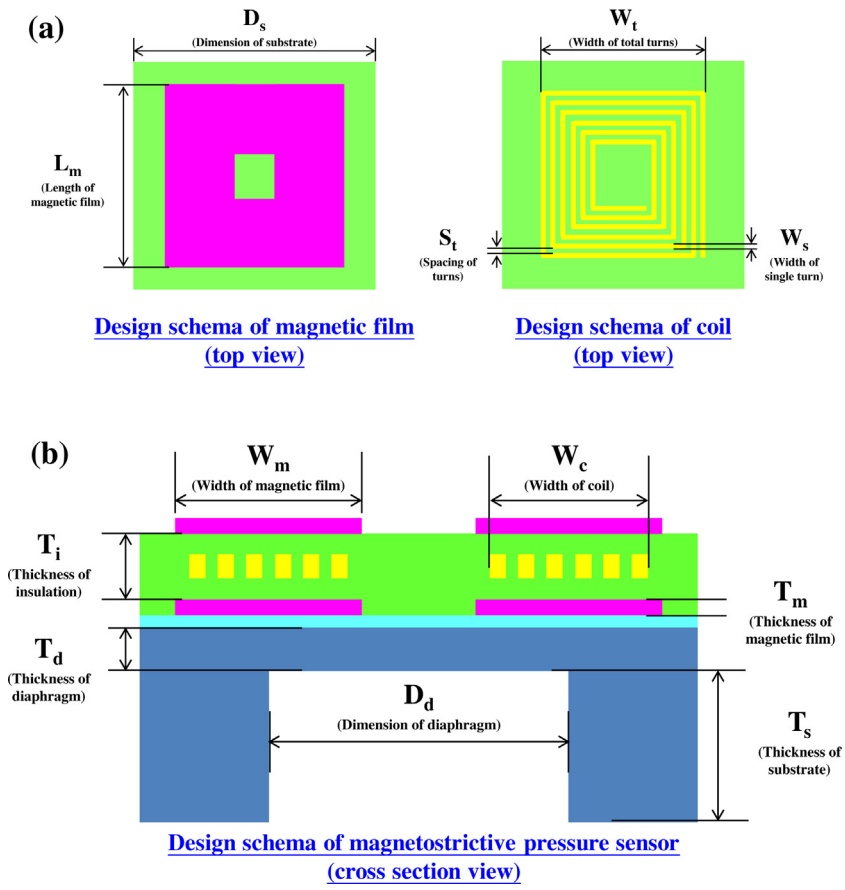

Fig. 2. The design schema of the magnetostrictive type pressure sensor, (a) top view, (b) cross section view.

In other words, due to the inverse-magnetostriction effect, the permeability of the CoFeB films will be changed by the pressure load. Thus, the permeability of the top and the bottom CoFeB magnetic films (μ_{top} and μ_{bot}) in Fig. 1(b) can be respectively determined from Eq. (3). The inductance of the planar coil sandwiched between the top and the bottom CoFeB films is expressed as [20],

$$L = \frac{\mu_0 \cdot {W_t}^2 \cdot N^2}{2 \cdot T_i + \frac{T_i}{\left({L_m}^2/{W_t}^2 - 1/2\right)} + \frac{\sqrt{2} \cdot W_t \cdot L_m}{8 \cdot \mu_{eq} \cdot T_m}} \quad (4)$$

where W_t (the width of total coil turns), T_i (the thickness of insulation), L_m (the length of magnetic film), and T_m (the thickness of magnetic film) are geometry parameters, as depicted in Fig. 2. Moreover, μ_0 is the vacuum permeability, N is the coil turns, and μ_{eq} is defined as the equivalent permeability which comes from the total coupling effect of μ_{top} and μ_{bot}. According to Eq. (3), μ_{top} and μ_{bot} would vary in accordance with the stress respectively on the top and the bottom magnetic films. Therefore, the equivalent permeability μ_{eq} before and after an applied pressure load will lead to the inductance change (from L_o to L_p) of the planar inductor. Consequently, the pressure load can be detected by the inductance change of the planar inductor (i.e. $L_p - L_o$). It is noticed from Eq. (1) that the inverse-magnetostriction effect is proportional to the stress on the magnetic films. Thus, the sensitivity of the proposed sensor could be enhanced if a higher stress is introduced on the magnetic films.

Fig. 2 also depicts the design parameters of the coil, magnetic films, insulation layers, and silicon diaphragm. The performances of the presented pressure sensor could be modulated by varying these design parameters using the fabrication processes. This study further proposed the pressure sensor design namely TP-N6 to demonstrate the presented approach. The TP stands for the application of tire pressure, and N6 marks the number of coil designs of 6 turns. The corresponding design parameters are summarized as, S_t = 10 μm, W_s = 10 μm, W_t = 650 μm, W_c = 110 μm, W_m = 210 μm, L_m = 750 μm, T_m = 0.2 μm, T_i = 10 μm, D_d = 540 μm, T_d = 20 μm, D_s = 1780 μm, and T_s = 400 μm. Note that the stress introduced by pressure load on the large area magnetic film will vary with the position. Thus, based on the design parameters described above, the stress distributions of different layers in the proposed magnetostrictive pressure sensor are determined by the commercial finite element method (FEM) software. Fig. 3 shows the distributions of von Mises stress for four different layers of the TP-N6 sensor under an applied pressure of 100 kPa. Note the stress introduced on the magnetic films could be modified by varying the dimensions of the Si diaphragm. After that, the inductance change of the proposed sensor is predicted from Eqs. (1)–(4).

The characteristics of the presented magnetostrictive pressure sensor could be modified by varying the designs for different applications. For instance, the sensor designs with 6 coil turns and 12 coil turns are listed in Table 1

. As indicated in Eq. (4), the inductance of planar coil is increased by the number of coil turns N. Moreover, the increasing of coil turns will also enhance the stiffness of the diaphragm, and further influence the stress distribution and magnitude of a deformed diaphragm. The FEM simulation results in Fig. 4(a and b) depict the distributions of von Mises stress on the top CoFeB film for

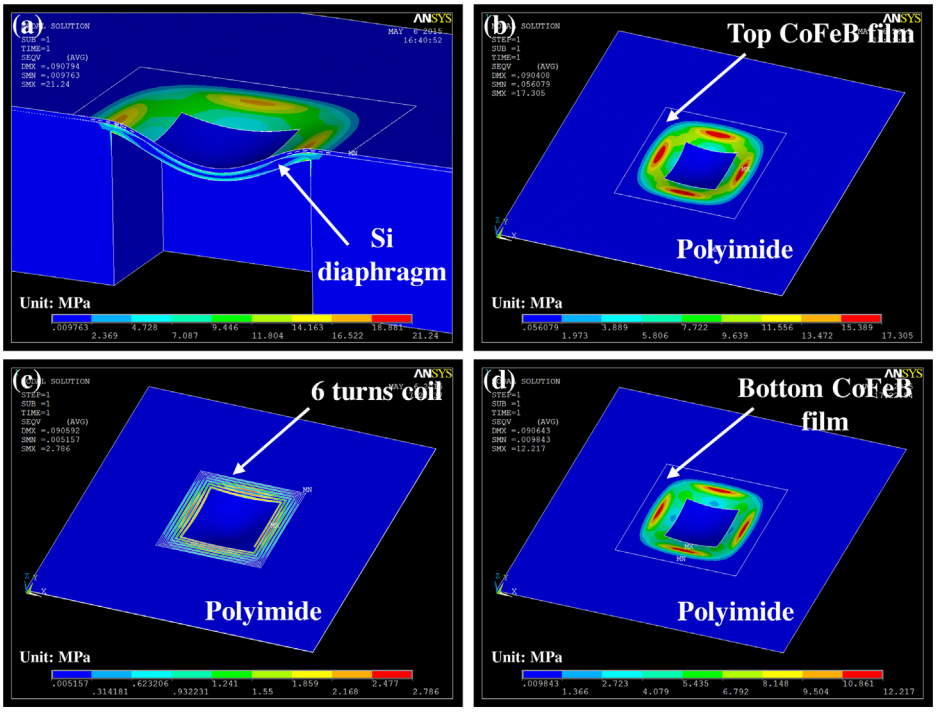

Fig. 3. The simulation results of stress distributions of the magnetostrictive type pressure sensor on, (a) Si diaphragm and planar inductor above it, (b) top magnetic film, (c) coil with 6 turns, and (d) bottom magnetic film.

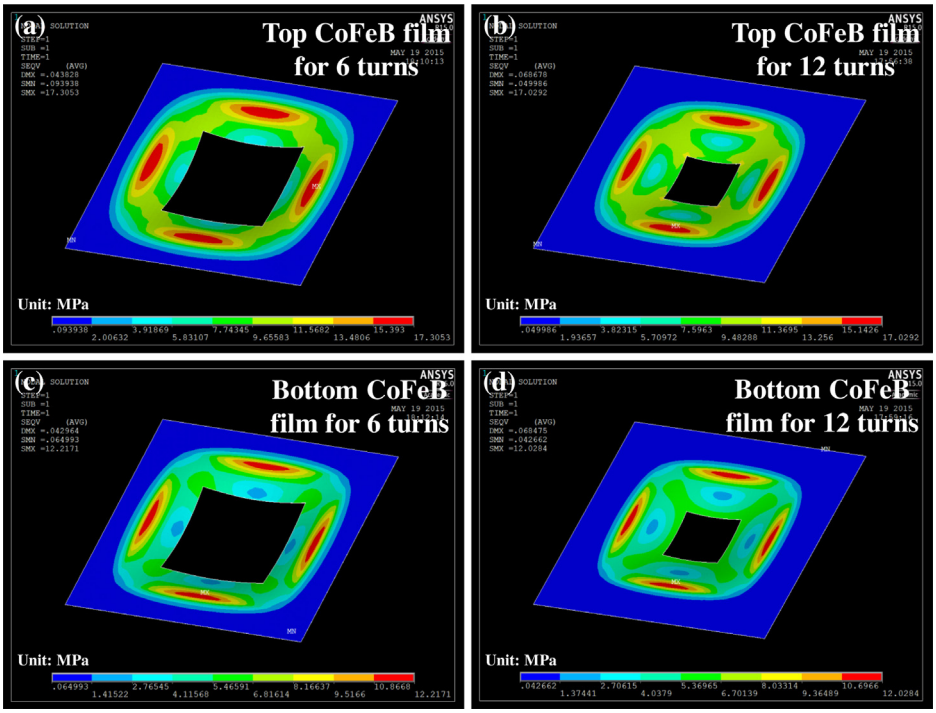

Fig. 4. The simulation results of stress distributions of the tire pressure sensor on, (a) top magnetic film for 6 coil turns, (b) top magnetic film for 12 coil turns, (c) bottom magnetic film for 6 coil turns, and (d) bottom magnetic film for 12 coil turns.

sensors of different magnetic coil turns (6 coil turns TP-N6, and 12 coil turns TP-N12). The pressure load is 100 kPa for the simulations. The results indicate that the maximum stress is decreased from 17.31 MPa to 17.03 MPa as the coil number increased from 6 to 12. Due to the lower stiffness of the diaphragm with 6-turn coil, the maximum stress introduced on its top magnetic film is higher. Similarly, the distribution and magnitude of the von Mises stress for the bottom CoFeB film are also influenced by the number of coil turns, as shown in Fig. 4(c and d). Table 2 further summarizes the predicted characteristics of TP-6 and TP-12 designs at a given pressure load (100 kPa). As a reference, the initial inductance and resistance of the air coil (metal coil only) are provided. In this

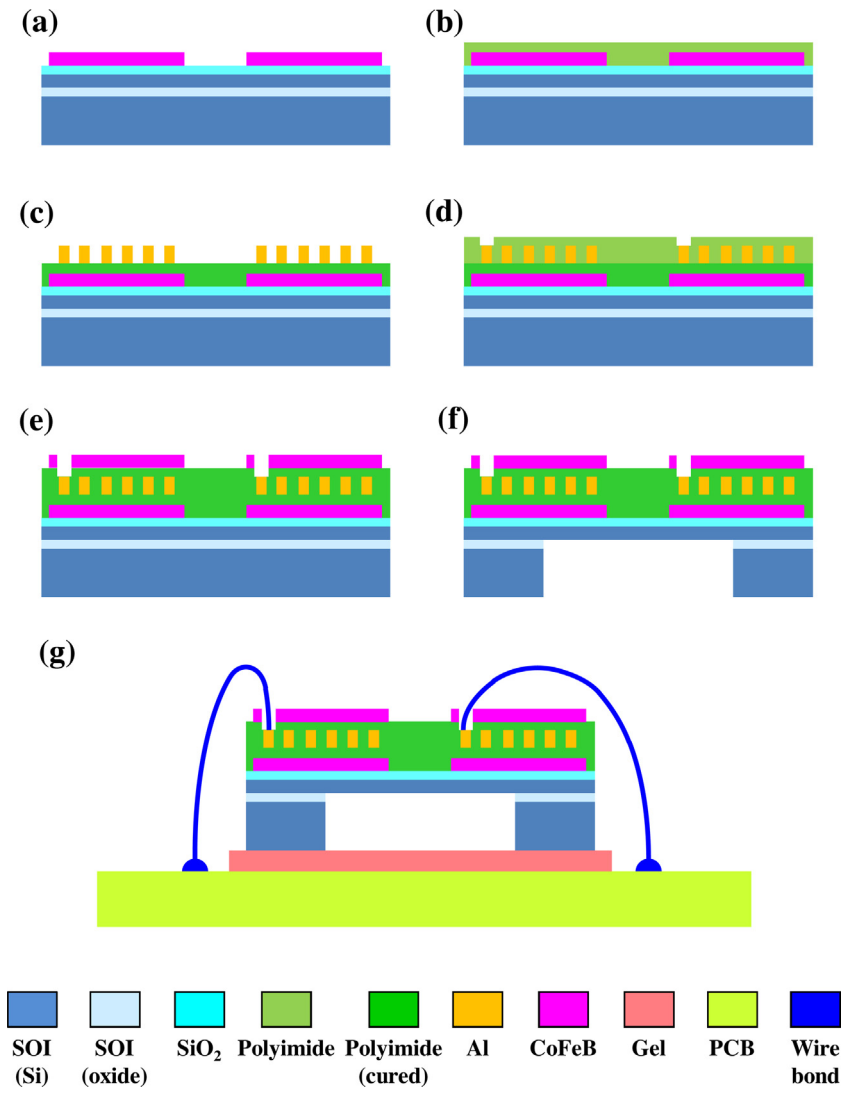

Fig. 5. The fabrication process flow of, (a) bottom magnetic film patterning, (b)–(d) coil patterning and polyimide curing, (e) top magnetic film patterning, (f) Si diaphragm defined by DRIE, and (g) bonding of the fabricated chip on a PCB.

Table 1
The design parameters of the magnetostrictive type pressure sensor based on the tire pressure sensing application with two coil designs.

Design parameters		TP-N6	TP-N12
Coil turns		6	12
Spacing of turns	S_t (μm)	10	10
Width of single turn	W_s (μm)	10	10
Width of total turns	W_t (μm)	650	770
Width of coil	W_c (μm)	110	230
Width of magnetic film	W_m (μm)	210	330
Length of magnetic film	L_m (μm)	750	870
Thickness of magnetic film	T_m (μm)	0.2	0.2
Thickness of insulation	T_i (μm)	10	10
Dimensions of diaphragm	D_d (μm^2)	540 × 540	540 × 540
Thickness of diaphragm	T_d (μm)	20	20
Dimension of substrate	D_s (μm^2)	1780 × 1780	1780 × 1780
Thickness of substrate	T_s (μm)	400	400

table, the stress and permeability changes induced by the 100 kPa pressure load is predicted first. After that, the inductance change of planar inductor, and the resolution and sensitivity of the pressure sensors are determined. The pressure change is detected by the proposed sensor with the readout signal (the inductance variation). Therefore, the minimum detectable pressure variation (i.e. resolution) is determined by the minimum readable inductance variation in this study (0.1 nH). In summary, the average stress on the CoFeB films of TP-N6 and TP-N12 designs are 3.34 MPa and 2.74 MPa, respectively. Thus, the sensitivity of TP-N6 design is higher than

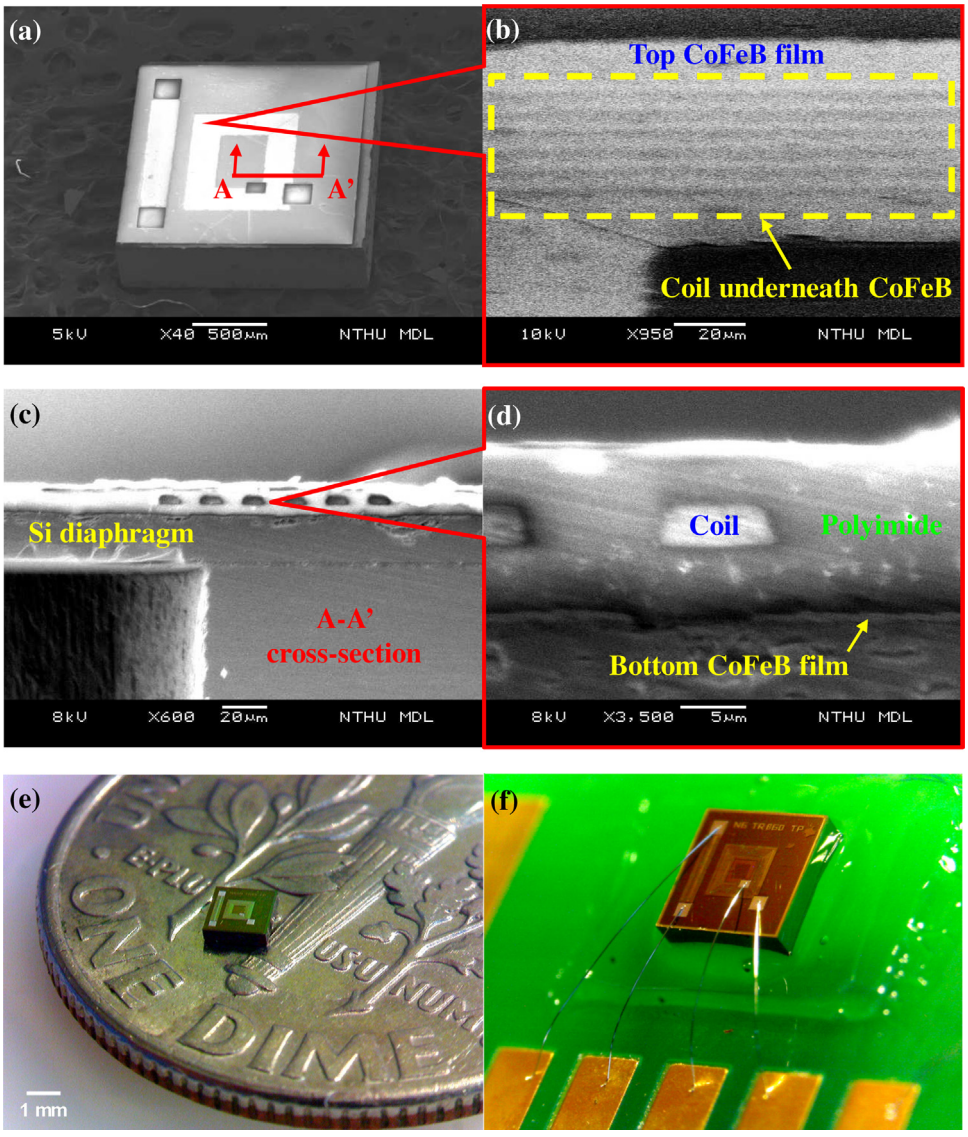

Fig. 6. The micrographs of fabrication results, (a) the proposed sensor chip, (b). the top magnetic film and the coil underneath it, (c) the cross-section view of the Si diaphragm, (d) The coil embedded in the polyimide with the bottom magnetic film underneath it, (e) the proposed sensor chip above one dime, (f) the sensor after wire bonding and packaging.

Table 2
The performance evaluation results of tire pressure sensors based on two designs of coil turns.

Evaluation results		TP-N6	TP-N12
Air coil	Initial inductance (nH)	37.30	104.36
	Resistance (Ω)	36.25	72.50
CoFeB magnetic film	Initial permeability (μ)	1382	1382
	Permeability@100 kPa load (μ)	1550	1517
	Maximum stress@100 kPa load (von Mises, in MPa)	17.31	17.03
	Average stress@100 kPa load (von Mises, in MPa)	3.34	2.74
Planar inductor	Initial inductance (nH)	55.60	232.60
	Inductance@100 kPa load (nH)	61.65	253.51
Pressure sensor	Sensitivity (%/kPa)	0.11	0.09
	Resolution (kPa)	1.65	0.48

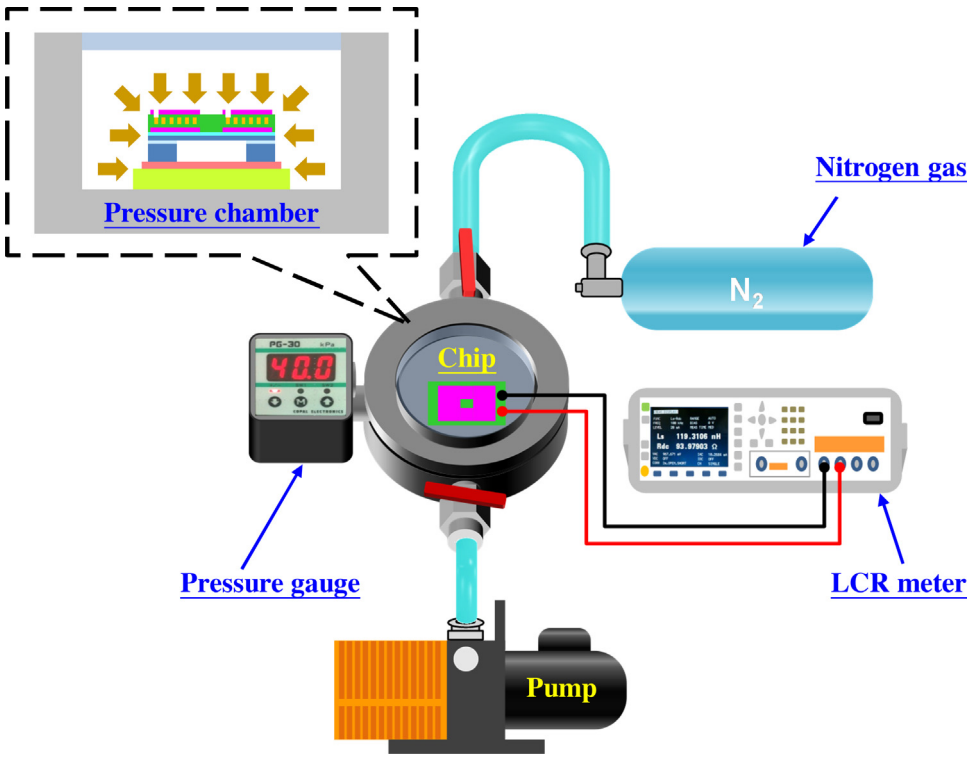

Fig. 7. The measurement setup of pressure facilities for the sensor performance testing.

that of the TP-N12 one. Moreover, the stress induced permeability and inductance changes are further determined by Eqs. (3) and (4), as indicated in Table 2. Note that the inductance is proportional to the coil turns to the power of two, as depicted in Eq. (4). Thus, the TP-N12 design which has a higher inductance variation could provide a better measurement resolution.

3. Fabrication and results

Fig. 5 illustrates the fabrication process steps to implement the pressure sensor proposed in this study. Firstly, the processes were performed on a SOI (silicon on insulator) wafer. Thus, the thickness of the deformable diaphragm in Fig. 1 can be precisely defined by the device layer of the SOI wafer. As shown in Fig. 5(a), a 1000 Å thick thermal oxide was grown as an insulation layer on the SOI wafer. After that, a 2000 Å thick CoFeB film was deposited and patterned to act as the bottom magnetic film for the planar inductor. As shown in Fig. 5(b), the polyimide layer (5 μm thick) was then coated onto the substrate. As illustrated in Fig. 5(c), after curing of the polyimide layer, the Al film (1 μm thick) was deposited and patterned to define the planar coil. The polyimide layer acts as an electrical isolation interface between the magnetic films and the planar coil. The planar Al coil was then covered with another polyimide layer. As shown in Fig. 5(d), the second polyimide layer (5 μm thick) was patterned to expose the bonding pads. The two bonding pads are respectively located at two terminals of the planar coil. After that, the polyimide layer was cured at 250 °C, as shown in Fig. 5(e). The curing temperature should be below 270 °C to prevent the crystallization of the CoFeB film. Note that the inverse-magnetostriction effect of the CoFeB film will be decreased by the crystallization. After the polyimide curing process, the second CoFeB film was deposited and patterned as the top magnetic layer. Next, as indicated in Fig. 5(f), the DRIE (deep reactive ion etching) was employed to perform the backside silicon etching to remove the handle Si layer of the SOI wafer and the buried oxide. Thus, the device Si layer was suspended to form the deformable diaphragm of the pressure sensor. Finally, as indicated in Fig. 5(g), the fabricated chip was bonded to a printed circuit board (PCB) using the gel. The wire bonding is also performed on PCB for the performance tests. After bonding, the chamber of pressure sensor is sealed from the ambient. Since the bonding is performed in atmosphere, the initial pressure inside the cavity is 1 atm.

The typical fabrication results are shown in Fig. 6. The scanning electron microscopy (SEM) micrograph in Fig. 6(a) displays a typical fabricated micro chip. The top CoFeB magnetic film and bonding pads are observed. The zoom-in SEM micrograph in Fig. 6(b) further depicts the CoFeB magnetic film and the planar coil underneath. The SEM micrograph in Fig. 6(c) shows the AA′ cross section indicated in Fig. 6(a) of a typical fabricated chip. The deformable diaphragm (formed by the device layer of the SOI wafer) and the planar Al coil embedded in the polyimide layers are observed. The zoom-in micrograph in Fig. 6(d) further depicts the stacking of the CoFeB magnetic film, polyimide isolation layers, and Al coil on top of the Si substrate. The micrograph in Fig. 6(e) shows the dimensions (1.78 mm × 1.78 mm × 0.4 mm) of a typical fabricated chip. Finally, Fig. 6(f) displays the fabricated chip after sealing and wire bonding on a PCB for the following tests.

4. Experiments and discussions

To demonstrate the presented concept, this study establishes the measurement setup consisting of a pressure chamber, a pressure gauge, a gas tank, a pump and a LCR meter, as shown in Fig. 7. After the packaging and wire bonding process, the entire PCB will be placed inside the chamber for the sensitivity testing, and the pressure load is monitored by a commercial pressure gauge. A positive

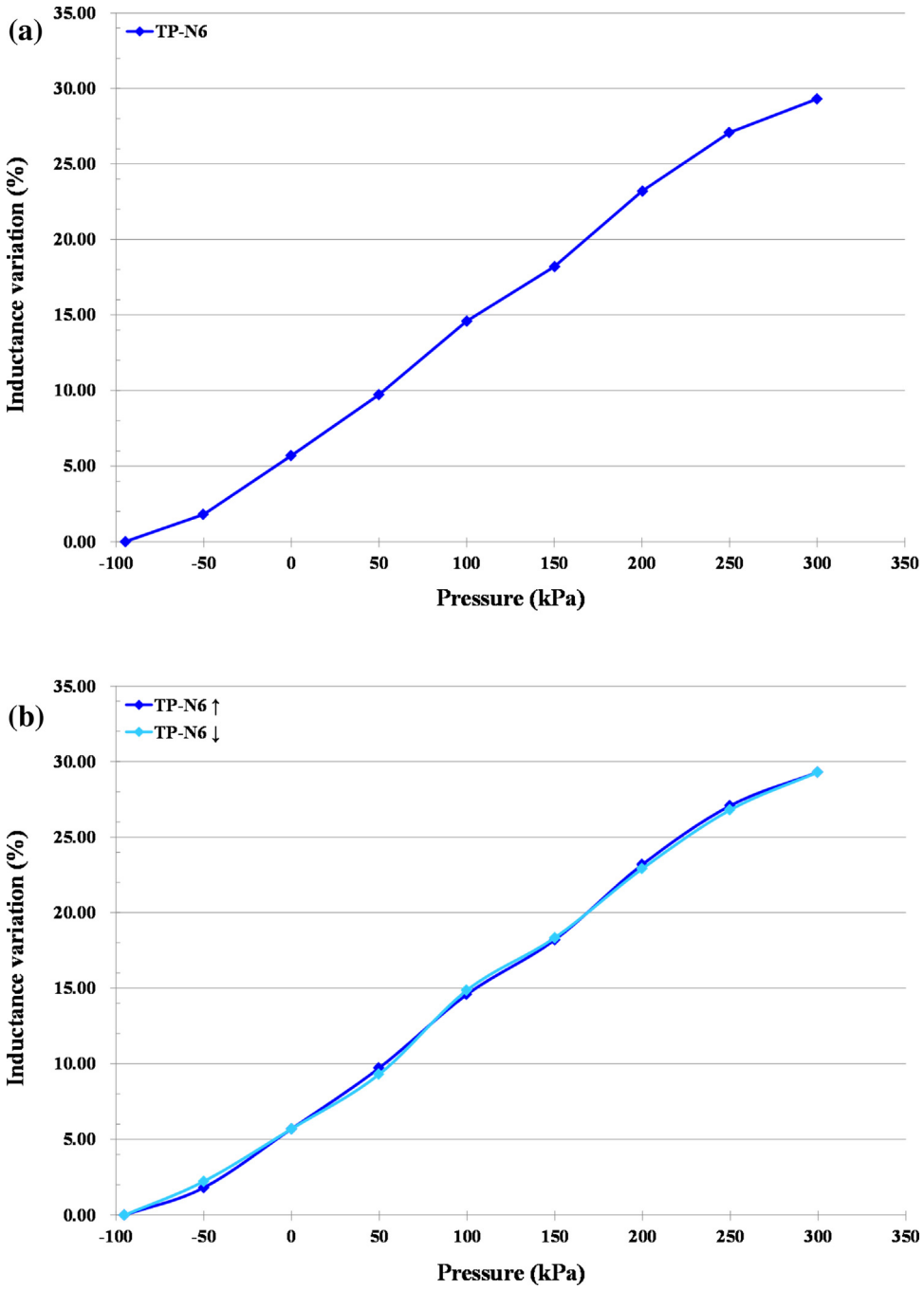

Fig. 8. The measurement results to show, (a) the sensitivity curve of the proposed sensor for the tire pressure sensing application, (b) the hysteresis phenomenon of the proposed sensor for the tire pressure sensing application.

pressure load is provided by the gas tank, whereas a negative one could be generated by the pump. Meanwhile, there is an electrical connection between the pressure sensor chip and the LCR meter. Once the inductance of the pressure sensor chip varies due to a pressure load, a corresponding inductance will be detected by the LCR meter. Consequently, the sensitivity could be evaluated from the relationship curve between the inductance variation and the pressure load. The typical measurement result in Fig. 8(a) shows the variation of the inductance change ($(L_p - L_o)/L_o$, in%) with the pressure load (in kPa) for the fabricated TP-N6 sensors. Measurement shows the sensitivity of TP-N6 pressure sensor is about 0.079 %/kPa, for the full span of 0–300 kPa (for the tire pressure sensor applications). Moreover, the corresponding gauge factor (the variation of the inductance change divided by the strain on magnetic film) is near 850. Note that the strain on magnetic film is determined from the FEM simulation. Fig. 8(b) further shows the hysteresis measurements of the TP-N6 pressure sensor. As indicated in Section 3, the initial pressure inside the chamber is the atmosphere after sealing. This study selected the vacuum as the starting point for the hysteresis testing. Thus, the base pressure of the hysteresis test is −100 kPa. Subsequently, the testing chamber was venting gradually with nitrogen up to 300 kPa, and then pumped down back to

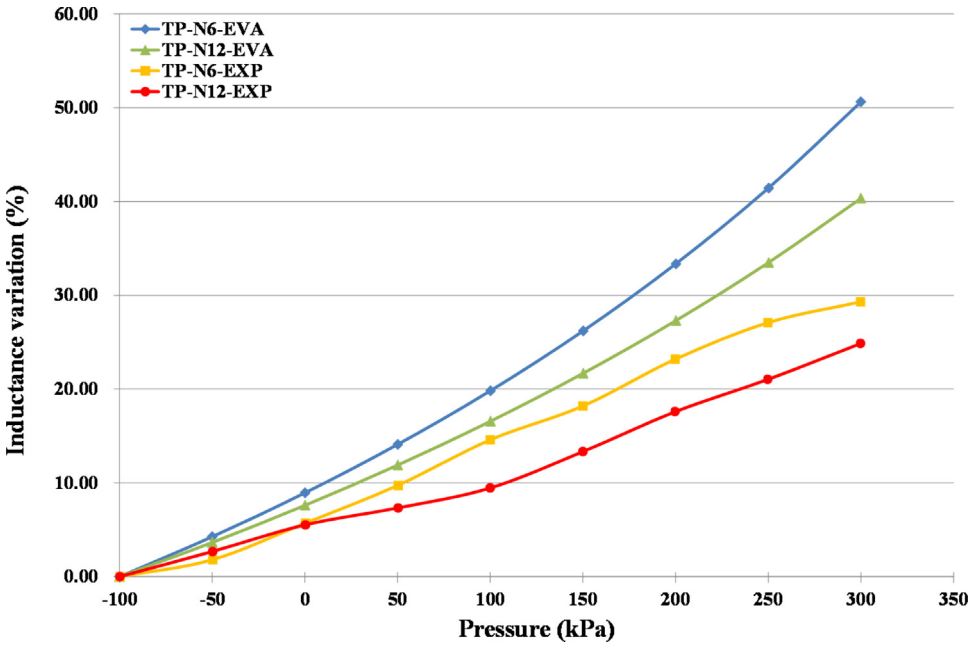

Fig. 9. The sensitivity curves of tire pressure sensors based on the experiment (EXP) and the evaluation (EVA) results.

the base pressure. Meanwhile, the inductance of the pressure sensor was recorded in this pressure controlling loop. As a result, the maximum deviation in the hysteresis loops of TP-N6 pressure sensor is about 0.42 % (as the pressure load is −50 kPa). To show the influence of the magnetic coil turns on the proposed design, the TP-N12 sensor discussed in Section 2 has also been fabricated and tested, as depicted in Fig. 9. Measurements show the sensitivity of TP-N6 design (0.079 %/kPa) is higher than that of the TP-N12 (0.064 %/kPa). The results agree reasonably with the simulations shown in figure. The difference may come from the residual stresses of the thin films after fabrication. Moreover, the resolution of TP-N12 design (0.85 kPa) is better than that of the TP-N6 (1.76 kPa). These results also agree reasonably with the results predicted in Table 2.

In this study, the CoFeB film is employed as the magnetostrictive film which results in the variation of magnetic anisotropy field H_s while stress is introduced, as mentioned in Eq. (1). As indicated in Eqs. (2)–(4), the inductance and permeability of magnetic film can also be changed by the initial anisotropy of magnetic field H_o. According to [19], the H_o can be modulated by varying the length to width ratio of magnetic film. To be more specific, higher length to width ratio would lead to higher magnetic anisotropic H_o. Thus, the in-plane pattern of the magnetic films (defined by the photolithography) would influence the H_o. To further investigate this characteristic, four geometry designs of the magnetic film as depicted in Fig. 10(a) are respectively implemented on TP-N12 sensor and then characterized. The length of these magnetic films (L_m) are all 870 μm. In addition to the single ring (SR) design presented in Fig. 2, this study also added three multi-ring (MR) designs of different line width (20 μm, 40 μm, and 60 μm). The gap between each line is 10 μm for these designs. The range of the length to width ratio of four designs are respectively: SR (2.64), MR-60 (5.17–14.5), MR-40 (6.75–21.75), and MR-20 (10.5–43.5). The single ring design has the lowest length to width ratio among all designs. On the other hand, the multi-ring designs may increase the length to width ratio, yet the leakage of the magnetic flux may occur at the gaps between the rings. Note that the gap between magnetic rings could be minimized by the process improvement to reduce the flux leakage. Measurements in Fig. 10(b) depict the M–H curves of the magnetic films with four ring pattern designs. The results were extracted by MOKE (Magneto-Optical Kerr Effect). According to Eqs. (2) and (3), the anisotropy field H_o is an important factor to affect the performance of the pressure sensor. Thus, the anisotropy fields of SR (H_{o1}), MR-60 (H_{o2}), MR-40 (H_{o3}), and MR-20 (H_{o4}) are marked in Fig. 10(b). Note that SR and MR-20 designs respectively show the smallest and largest H_o among all samples. In other words, the pressure sensor with SR design would have the highest sensitivity among all ring designs, whereas the MR-20 design would provide the lowest sensitivity. To further examine the influence of the CoFeB film pattern on the sensor performance, four ring designs are further fabricated and employed as the magnetic sensing film underneath the coil, as shown in Fig. 10(c). The comparison is focused on the geometry designs of the bottom magnetic film. Therefore, except the bottom film, the other design parameters of the pressure sensor, such as the number of coil turns, the geometry of the top magnetic film, or the diaphragm size, are the same for a fair comparison. For instance, the diaphragm is 540 μm × 540 μm in dimensions and the planar coil is 12 turns. Typical measurement results in Fig. 11 show the variation of the inductance change with the pressure load for pressure sensors employed the four ring designs. In comparison, the single-ring design provides the highest sensitivity (0.064 %/kPa) as well as gauge factor (611) among all designs. As for the multi-rings designs, MR-60, MR-40, and MR-20 respectively have the gauge factors of 179, 111, and 55. The results agree well with the prediction from design.

5. Conclusions

This study proposes a design concept of the pressure sensor based on the inverse-magnetostriction effect and inductive sensing technique. By varying the design parameters of the planar inductor, such as the coil turn number and the magnetic film geometry, the gauge factor of the sensor could be tuned. Moreover, in this study, the CoFeB film is employed as the magnetostrictive film which results in the variation of magnetic anisotropy field

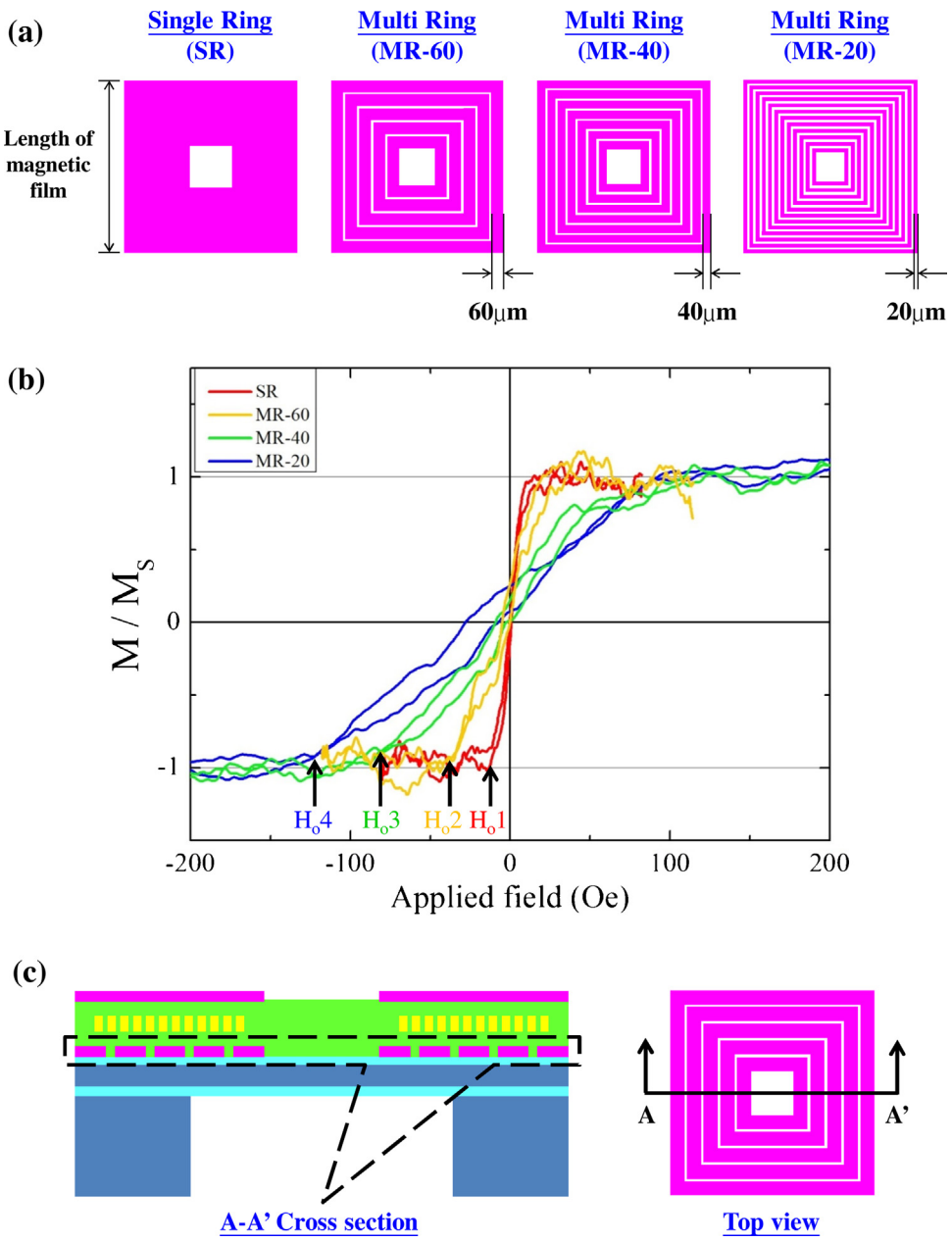

Fig. 10. (a) 4 designs on the shape of magnetic films with the same length of magnetic film, (b) The M–H curves of the magnetic films with 4 shape designs, (c) The proposed sensor employs the magnetic film shape design of MR-60.

H_s while stress is introduced, as mentioned in Eq. (1). The initial anisotropy field H_o could also be adjusted during the film deposition. To demonstrate the feasibility of the proposed design concept, the planar inductors consisted of the designs with two different coil turns and four different CoFeB patterns have been fabricated. The sensitivity of the fabricated chips with various planar inductor designs has been characterized. According to the measurement results, the gauge factor is modified from 55 to 852 by the design parameters of the planar inductor. Note that the gauge factor of 852 is about 12 times the factor of the general piezoresistive type pressure sensor. In summary, this study demonstrates the design and the feasibility of the magnetostrictive type pressure sensors. The design parameters in Section 2 can be further investigated to enhance the performances of the magnetostrictive type pressure sensors. The presented magnetostrictive type pressure sensor is a strain induced sensing device. The same sensing mechanism can be further expanded to the applications of the accelerometer, microphone, etc. The existing of the planar coil also offers the potential to integrate with the inductance reading circuitry for wireless transmission applications.

Acknowledgements

The authors would like to thank Delta Electronics Inc. for the relative manufacturing and test facilities. This work was supported in part by the National Science Council of Taiwan under the grant of NSC-102-2218-E-007-003, NSC 102-2622-E-007-014-MY3, and the grant for “the Toward World-Class University Project from National Tsing Hua University, Taiwan”.

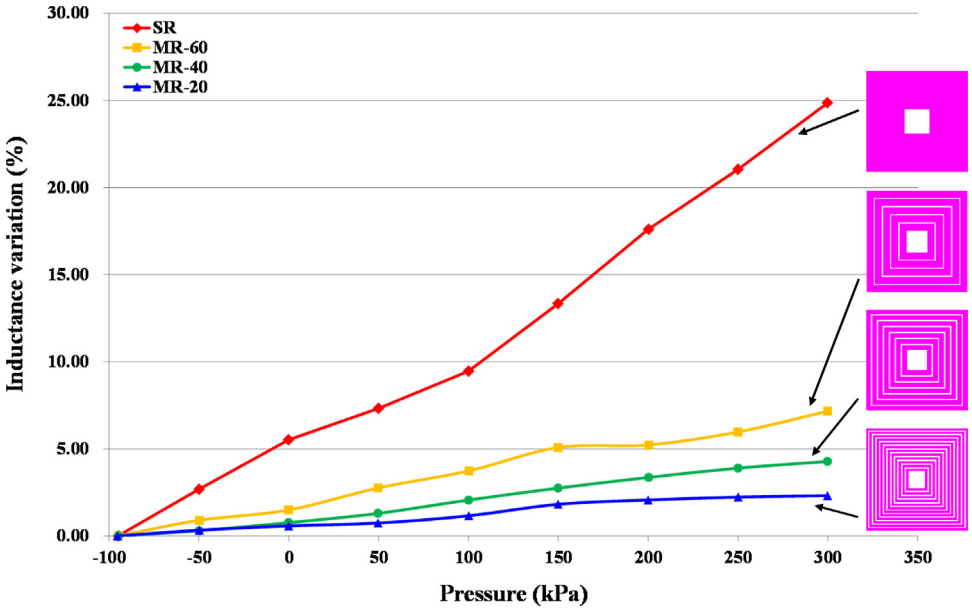

Fig. 11. The measurement results to show the sensitivity curves of the proposed sensor with 4 magnetic film shape designs.

References

[1] W.P. Eaton, J.H. Smith, Micromachined pressure sensors: review and recent developments, SPIE 3046 (1997) 30–41.
[2] K.N. Bhat, M.M. Nayak, MEMS pressure sensors: an overview of challenges in technology and packaging, J. Inst. Smart Struct. Syst. 2 (2013) 39–71.
[3] G.T.A. Kovacs, Micromachined Transducers Sourcebook, McGraw-Hill, 1998.
[4] V. Musser, J. Suski, J. Goss, E. Obermeier, Piezoresistive pressure sensors based on polycrystalline silicon, Sens. Actuators A 28 (1991) 113–132.
[5] O.N. Tufte, E.L. Stelzer, Piezoresistive properties of silicon diffused layers, J. Appl. Phys. 34 (1963) 313–318.
[6] C.S. Schneider, P.Y. Cannell, K.T. Watts, Magnetoelasticity for large stresses, IEEE Trans. Magn. 28 (1992) 2626–2631.
[7] K. Yamamoto, S. Takada, T. Sasaki, Change of the magnetization due to a change of stress after demagnetization in amorphous ribbon, IEEE Trans. Magn. 31 (1995) 3778–3780.
[8] M.J. Sablik, A model for asymmetric in magnetic property behavior under tensile and compressive stress in steel, IEEE Trans. Magn. 33 (1997) 3958–3960.
[9] D. Meyners, T.V. Hofe, M. Vieth, M. Ruhrig, S. Schmitt, E. Quandt, Pressure sensor based on magnetic tunnel junctions, J. Appl. Phys. 105 (2009), 07C914.
[10] M. Löhndorf, S. Dokupil, M.T. Bootsmannb, A. Malavé, M. Rührig, L. Bär, E. Quandt, Characterization of magnetostrictive TMR pressure sensors by MOKE, J. Magn. Magn. Mater. 316 (2007) e223–e225.
[11] A.B. Amor, T. Budde, H.H. Gatzen, A magnetoelastic microtransformer- based microstrain gauge, Sens. Actuators A 129 (2006) 41–44.
[12] X. Xu, M. Li, J. Hu, J. Dai, W. Xia, Strain-induced magnetoresistance for novel strain sensors, J. Appl. Phys. 108 (2010), 033916.
[13] D. Wang, C. Nordman, Z. Qian, J.M. Gaughton, J. Myers, Magnetostriction effect of amorphous CoFeB thin films and application in spin-dependent tunnel junctions, J. Appl. Phys. 97 (2005), 10C906.
[14] R.C. O'Handley, Magnetostriction of transition-metal metalloid glasses: temperature dependence, Phys. Rev. B 18 (1978) 930–938.
[15] E.G. Bakhoum, M.H.M. Cheng, High sensitivity inductive pressure sensor, IEEE Trans. Instrum. Meas. 60 (2011) 2960–2966.
[16] W. Yang, Q. Yang, R. Yan, W. Zhang, X. Yan, F. Gao, W. Yan, Dynamic response of pressure sensor with magnetic liquids, IEEE Trans. Appl. Supercond. 20 (2010) 1860–1863.
[17] P.J. Chen, S. Saati, R. Varma, M.S. Humayun, Y.C. Tai, Implantable flexible coiled wireless intraocular pressure sensor, IEEE MEMS 2009 (2009) 244–247.
[18] S.L. Martínez, R. Giannetti, J.L.R. Marrero, B. Tellini, Design of a system for continuous intraocular pressure monitoring, IEEE Trans. Instrum. Meas. 54 (2005) 1534–1540.
[19] B.D. Cullity, C.D. Graham, Introduction to Magnetic Materials, John Wiley & Sons, Inc., Hoboken, New Jersey, 2009.
[20] K. Kawabe, H. Koyama, K. Shirae, Planar inductor, IEEE Trans. Magn. 20 (1984) 1804–1806.

Biographies

Heng-Chung Chang was born in Taichung, Taiwan. In 2001, he received his B.S. degree in mechanical engineering as a member of the Phi Tau Phi Scholastic Honor Society from Chang Gung University, Taiwan. He received his M.S. degree from Power Mechanical Engineering Department of National Tsing Hua University (Taiwan) in 2003. As a researcher in the corporate RD center of Delta Electronics, Inc., he focused on the MEMS sensors development since 2003 until 2011. In 2014, he was a visiting scholar at Tokyo Institute of Technology, Japan. He is currently a Ph.D. candidate in the Power Mechanical Engineering Department of National Tsing Hua University, Taiwan. His research interests include sensor applications, actuator designs, and processes integration.

Sheng-Chieh Liao was born in Taichung, Taiwan. He received his B.S. degree from Department of Materials Science & Engineering, National Tsing Hua University in 2008. He continued to be a Ph. D student with Prof. Chih-Huang Lai as the advisor. He works on the soft ferromagnetic films for inductor, exchange coupling with bismuth ferrite, and epitaxial magnetic nanostructures grown with pulsed laser deposition. He has published 13 SCI papers.

Hsieh-Shen Hsieh received his B.S. and M.S. degrees in mechanical engineering respectively in 2000 and 2002 from National Cheng Kung University, Tainan, Taiwan. He received his Ph.D. degree in power mechanical engineering from National Tsing Hua University (Taiwan) in 2012. From 2003 to 2010, he was a researcher in the corporate RD center of Delta Electronics, Inc., in which he was in charge of sensor design based on MEMS technology. In 2011, he was a visiting scholar at University of California Berkeley, California. He is currently a department manager at magnetic device business group, Cyntec Co., Ltd.

Jung-Hung Wen received his M.S. degree in Electronic engineering in 1996 from Chung-Yuan Christian University, Taoyuan, Taiwan. He is currently a Ph.D. candidate in Institute of NanoEngineering and MicroSystems at the National Tsing Hua University (Taiwan). His research interests include monolithic CMOS-MEMS device design and system implementation.

Prof. Chih-Huang Lai was born in Tainan, Taiwan. He received his Ph.D. degree from Stanford University in 1997. He joined the Department of Materials Science & Engineering in National Tsing Hua University, Taiwan in 1999, and now he is a chair professor, as well as the chair of magnetic society, IEEE Taipei section. He works on the magnetic thin film, especially for the application purposes of MRAM, recording media, magnetic sensors. He received two SCI outstanding research awards in 2010 and 2013. He published more than 140 SCI journal papers and 16 patents in magnetic field.

Weileun Fang (F'15) was born in Taipei, Taiwan. He received his Ph.D. degree from Carnegie Mellon University in 1995. His doctoral research focused on the determining of the mechanical properties of thin films using micromachined structures. In 1995, he worked as a postdoctoral research at Synchrotron Radiation Research Center, Taiwan. He joined the Power Mechanical Engineering Department at the National Tsing Hua University (Taiwan) in 1996, where he is now a Distinguished Professor as well as a faculty of NEMS Institute. In 1999, he was with Prof. Y.-C. Tai at California Inst. Tech. as a visiting associate. His research interests include MEMS with emphasis on micro fabrication/packaging technologies, CMOS MEMS, CNT MEMS, micro optical systems, micro sensors and actuators, and characterization of thin film mechanical properties. Prof. Fang has published more than 140 SCI journal papers, near 250 international conference papers, and 80 patents (all in MEMS field). He is now the Editor-in-Chief of JMM, the Board Member of IEEE TDMR, and the Associate Editor of IEEE Sensors J., and Sensors and Actuators A. He served as the chief delegate of Taiwan for World Micromachine Summit (MMS) from 2008 to 2012, and chaired the MMS 2012. He also served as the TPC of IEEE MEMS conference, the EPC of Transducers conference, and the regional co-chair as well as TPC chair of IEEE Sensors conference. He has become the member of international steering committee of Transducers from 2009. Moreover, he also serves as a technical consultant for many MEMS companies in Taiwan.Dr. Fang is a member and Fellow of the IEEE, and the IOP (Institute of Physics, UK).